Fabrication and characterisation of TiO_2 anti-reflection coatings with gradient index

Li Tian[1] ✉, *Ling Li*[1], *Min Wu*[2]

[1]*School of Astronautics, Harbin Institute of Technology, Harbin 150001, Heilongjiang Province, People's Republic of China*
[2]*Shanghai Solar Energy Research Center, Shanghai 200241, People's Republic of China*
✉ *E-mail: tianli@hit.edu.cn*

Published in Micro & Nano Letters; Received on 9th June 2017; Revised on 17th July 2017; Accepted on 27th July 2017

Nano-textured anti-reflection (AR) films are designed elaborately to improve the transmittance character and to reduce the surface reflection loss. This work reports the gradient-index titanium dioxide (TiO_2) AR coatings (ARCs) with the thickness of 50–400 nm, which was deposited by radio-frequency magnetron sputtering-assisted with the oblique-angle deposition technique on the low-iron glass substrates. The technological parameters related with this deposition were discussed such as the base pressure and target–substrate distance, as well as the vapour incident angle. Then, optical characteristics of the graded-index coating were discussed. An ellipsometric model was built to account for the structural and optical differences. The optimal thickness of the TiO_2 ARC was about 250 nm. It exhibited a higher transmittance at the visible light regions over a large wavelength range than that of the primitive glass substrate. The value of refractive index for the TiO_2 ARC was 2.245 at the wavelength of 632.8 nm.

1. Introduction: Conventional planar anti-reflection coatings (ARCs) whether monolayer or multilayer thin films are designed to provide excellent AR performance within limited ranges of angles of incidence and wavelength [1–4]. While as a surface-relief optics technology based on very large-scale integration fabrication techniques (primarily photolithography and etching), binary optics technology allows the creation of novel, unconventional optical devices for refractive optical elements and enable the fabrication of unique wavefront engineering devices from X-ray to infrared wavelength [5, 6].

ARCs have evolved into highly effective reflectance and glare reducing components because of their wide application as various optical and opto-electrical equipments, packaging materials in photovoltaic or display etc. However, the fact cannot be neglected that the adsorption of organic contaminants from the ambient atmosphere, particularly in outdoor applications, made the performance deteriorated and affected its long-term usability. Titanium dioxide (TiO_2) is a large bandgap semiconductor. Owing to its better characters such as high transmittance in visible spectral range, TiO_2 has been widely used in multilayer optical filters, optical waveguides and other application [7]. While the most distinguished feature about TiO_2 is its more robust and durable photocatalytic self-cleaning character for the breakdown of organic substances under ultraviolet (UV) illumination. However typically, its high refractive index ($n_{TiO_2} > 2.5$) also poses a major challenge for its application, especially as ARCs [8].

To overcome the conflicting requirements for low refractive index and high transmittance, sub-wavelength nano-texturing ARC layer is a promising new approach to enhance the light transmittance for advanced light trapping purpose in different device geometries. Various structures including randomly or periodically textured surfaces, nanoparticle arrays and plasmonic nanostructures have been investigated both theoretically and experimentally [7–10]. Majorities of fabrication methods have been developed such as vapour–liquid–solid, solution–liquid–solid, metal-assisted chemical etching, nano-imprint lithography, oblique-angle deposition (OAD), atomic layer deposition (ALD) technique etc [9–19]. Xi *et al.* fabricated five-layered graded-index films with TiO_2/SiO_2 nanorods on aluminium nitride substrate by OAD at a vapour incident angle of 87° [11]. The minimum index was reported to be 1.05 and the lowest reflectance was only 0.1% at an incident angle of 30°. Pushpa *et al.* reported an optimised silicon nanoholes array texture surface in combination with the surface and bottom-of-a-trench gold (Au) nanoparticles array, which producing a strong field enhancement effect on the substrate leads to higher optical absorption [12]. This research team also employed sub-micrometre pillar array textured aluminium oxide as a surface passivation layer fabricated with ALD technique, then got the broadband omnidirectional AR effects along with the light trapping property of the surface and the excellent passivation quality [13].

In this Letter, we report a kind of TiO_2 ARC with graded index and its fabrication process. ARCs were deposited using the radio-frequency (RF) magnetron sputtering (MSP) combining with OAD method, where the graded-index is realised by controlling the deposition parameters of the source incident angle and the distance from the centre of target to the centre of substrate holder. With this approach, the refractive index of the TiO_2 coating varied gradually, exhibited enhanced anti-reflectivity. The nanostructure and morphology of the thin film would be analysed by scanning electron microscope (SEM) images to know the effect of substrate position on the structure and optical properties. A strict experimental analysis about the annealing characters would be addressed to comprehend the different parameters involved in the optical transmittance response of the TiO_2 thin films.

2. Experimental results: The conventional vacuum-based fabrication approaches are typically relying on glancing AD or OAD technique to produce precise nanostructures from a wide range of materials [11, 16, 18].

In this Letter, the gradient-index TiO_2 coatings were deposited on the low-iron glass substrate (cut into 20 mm × 20 mm sections). The target of the sub-stoichiometric TiO_{2-x} (Φ49 mm) was used in the TiO_2 thin-film deposition, whose thicknesses concluded 40–250 nm were fabricated with the JZCK-400 RF MSP equipment at a specific incident angle β, as shown in Fig. 1*c*. The base pressure was 9.4×10^{-4} Pa, the flux ratio of argon and O_2 was 2 : 1 at 0.57 Pa sputtered pressure. The centre distance from the TiO_2 target to substrate holder was 75 mm, the deposition temperature was 400 K at a constant power of 190 W in 2 h. The deposition material began to deposit on the surface at a rate of 0.05 nm/s. The thickness and deposition rates of TiO_2 were monitored by a quartz crystal microbalance directly facing the vapour source. The detailed description about the process of the film deposition was in a previous work [20].

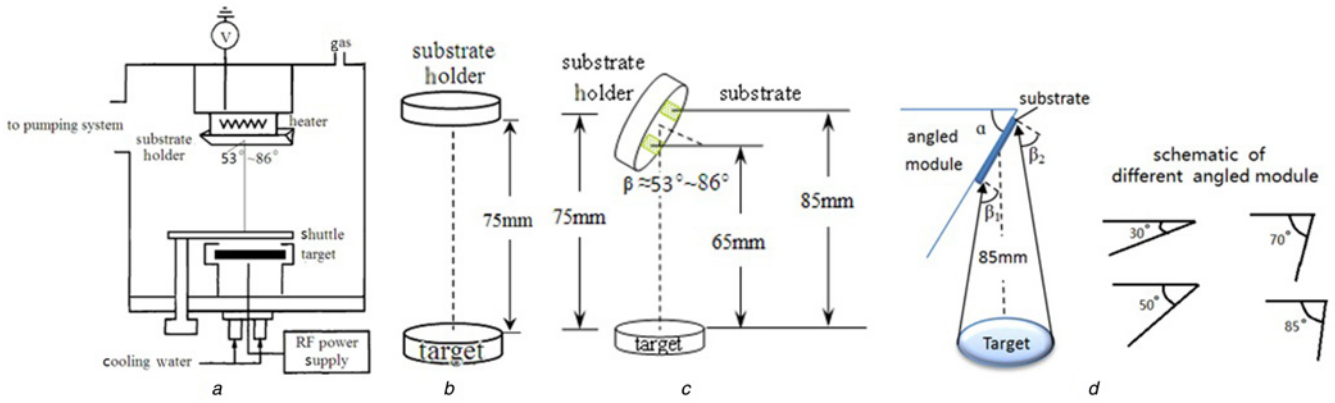

Fig. 1 *Schematic of RF MSP furnace assisted with OAD technique*
a MSP deposition
b Normal deposition
c OAD-assisted deposition
d Vapour incident angles

In the coatings preparation, the process parameter variables involved in time, vapour incidence angle, target–substrate distance material selection etc. As the substrate holder is parallel with the target holder in the conventional deposition, here we designed a series of different angled module to replace the original substrate holder. The substrate is mounted on the angled module ($a = 30°$, 50°, 70° and 85°) with respect to the conventional incidence deposition material vapour flux. The distance between the regular horizontal rotation holder and the target source was 75 mm. The deposition angles from such a large area of source (ϕ 49 mm), a preferential direction of arrival can be preserved to some extent, as shown in Fig. 1*d*. The TiO molecular arrived at the surface of the substrates at the range of 53−85° statistically, thereby inducing the growth of OAD thin films with the nano-textured structures [11].

It has been established by Fresnel that the angle of incidence plays a decisive role in the determination of reflectance [8]. The pictures of the as-deposited TiO_2 coatings were taken at different azimuth angles, as shown in Fig. 2.

From the photoshooting at elevation view, the left sample was placed at the target–substrate distance of 85 mm during the deposition, while the right one was placed at the target–substrate distance of 65 mm. They were fabricated in the same processing batch, but they exhibited the different colours to the naked eye, which illustrated their different reflectance features. As the change of shooting azimuth, the surface reflection colour of the TiO_2 coatings also changed. Especially, when the photograph was shooting at the angle of 45° in the North side, both of the TiO_2 coatings showed nearly white colour. At a particular shooting angle, there was no visible light reflected to our naked eyes. The coatings are almost completely transparent, and we can see the filter paper clearly.

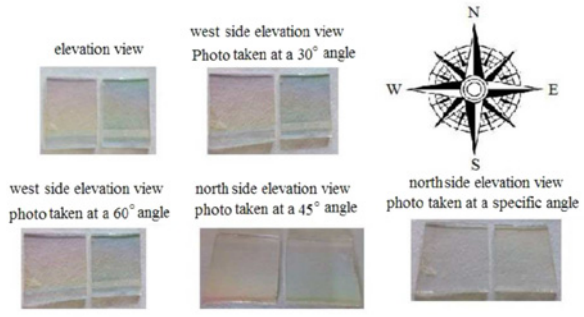

Fig. 2 *Pictures of the as-deposited TiO2 coatings at different shooting angles*

While OAD films had been reported to be anisotropic in previous research [16]. The reflected characteristics of the TiO_2 ARC coatings fabricated by our MSP processing also had the properties of optical anisotropy, which indicated that the AR performance changed with the incident angle.

To study the effect of annealing on the crystallisation of the TiO_2 thin film and compare the transmittance properties, we annealed the six TiO_2 film samples in air at the temperatures of 623, 673, 723 and 773 K for 2 h, respectively. All as-deposited as well as heat-treated films were analysed. As the functional components to increase light transmission, moreover to eliminate unwanted reflections and glare, ARC and surfaces have enabled the increasing performance of optical components.

3. Results and discussion: We fabricated 11 TiO_2 thin-film samples for the characterisations. The nanostructure and morphology of the TiO_2 thin film were performed with an SEM (SEM, VEGA3 SBH, TESCAN China, Ltd.) and CSPM5500 atomic force microscope (AFM, Being Nano-Instruments Ltd.), as shown in Fig. 3. Samples were Au-coated previous to SEM observations. Fig. 3*a* exhibited top-view SEM images of the normal sputtered TiO_2 films after post-treatment at 753 K for 2 h, the small nucleation sites formed, and the islands of material distributed randomly on the surface of the glass substrate. Then, the pre-deposited TiO_2 on the glass is used as the second-deposition substrate. Fig. 3*b* exhibited the sputtering TiO_2 films assisted with the OAD technique. Owing to height variations and the angle of deposition, the molecular of TiO_2 was self-organised along the direction of incident vapour flux. With the increasing incident time, the porosity of the film increased due to the self-shadowing effect, then began to grow into nanocolumnar structures. The average surface roughness had been calculated $R_{AFM} = 22.5$ nm from the topographical data.

The test of light transmittance was performed with a 755B UV–visible (UV–vis) spectrophotometer (Shanghai Jinghua Company, China) in transmission mode. Transmittance of the surface of a material is its effectiveness in transmitting radiant energy, which is the fraction of incident electromagnetic power transmitted through a sample [21]. Light transmittance of coated glass is one of the important indexes of optical properties. The UV–vis spectra of the as-deposited films, as well as for the annealed films, were collected in the spectral range of 250–1000 nm at indoor temperature. All of the transmittance tests were performed in condition that the incident light was normal to the surface of glass substrate. The transmittance spectra for the samples obtained in the same or different deposition run were shown in Figs. 4*a–d*.

doi: 10.1049/mnl.2017.0408

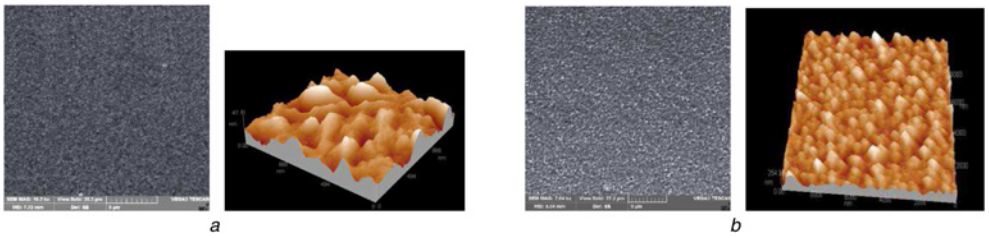

Fig. 3 *Top-view SEM images of TiO_2 films*
a TiO_2 coatings ($a = 0°$)
b TiO_2 coatings ($a = 85°$)

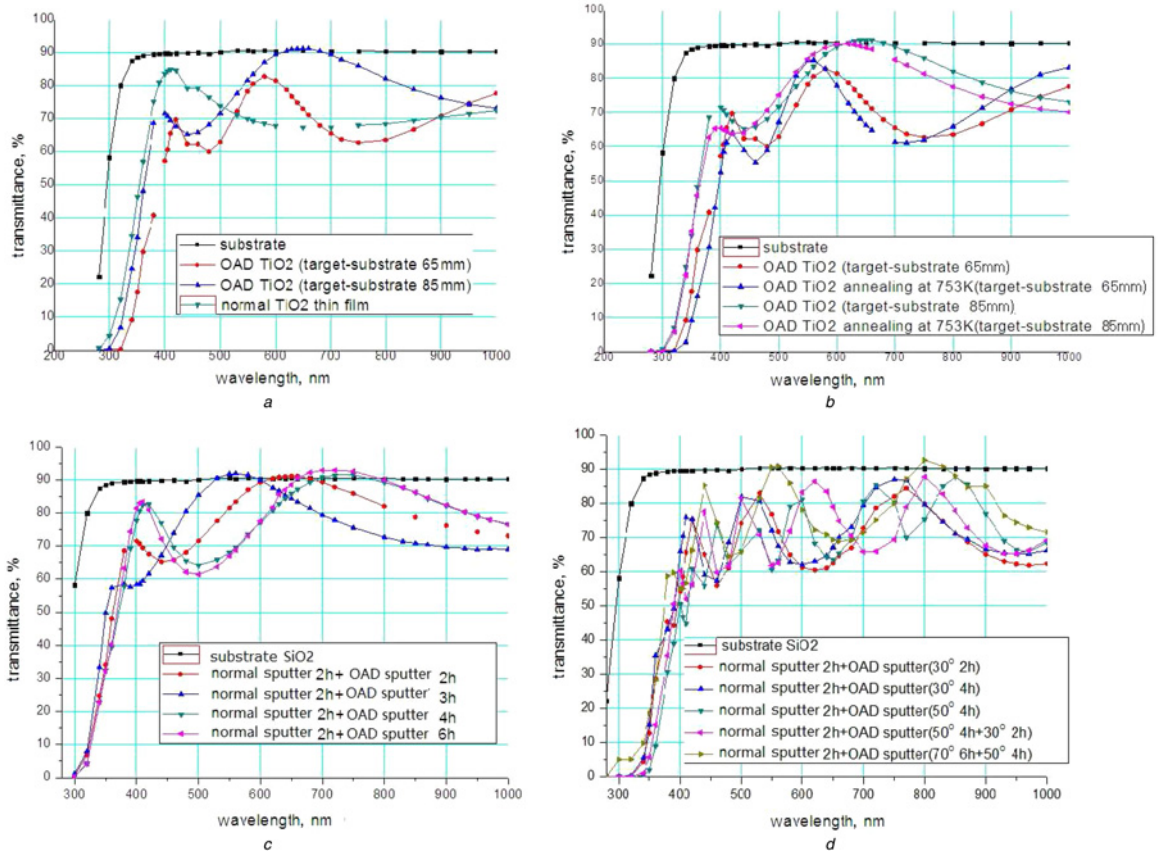

Fig. 4 *UV–vis spectrum of deposited TiO_2 coating*
a TiO_2 coatings deposited with the 85° module (before heat treatment)
b Same sample before and after annealing at 753 K
c TiO_2 coatings deposited with the 85° module at different deposition time lengths
d TiO_2 coatings deposited at the different incident angles and deposition time lengths

The TiO_2 coatings were deposited with the 85° module with which the incident angle of TiO_2 vapour molecular was calculated to be about 68.6-85°, as indicated in Fig. 1*d*. All the experimental transmittances through uncoated low-iron glass substrate were in black colour. Fig. 4*a* showed the TiO_2 coatings with regular sputtering technique (in green colour) and TiO_2 coatings with OAD-assisted sputtering technique (the 85 mm target–substrate distance in blue colour and the 65 mm target–substrate distance in red colour). Compared to the uncoated substrate, the transparency of the films exhibited a sharp decrease in the wavelength range of 300–400 nm. Moreover, the normal-deposited TiO_2 coatings exhibited a band-filter nature in the wavelength range of 380–550 nm. While the transmittance of TiO_2 coatings (OAD-assisted deposited) had the better transmittance character. The film deposited at 85 mm target–substrate distance exhibited the best optical performance, so that later work was based on this parameter. The peak of transmittance was up to 91.1% in air mass 1.5 (AM1.5) atmosphere, which

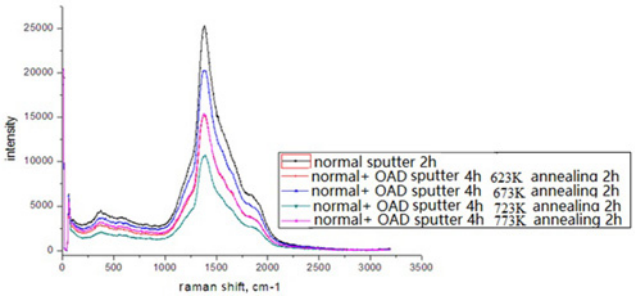

Fig. 5 *Raman spectrum of deposited TiO_2 coating*

was increased by 0.77% than the primitive of the glass substrate (90.4%).

Fig. 4*b* plotted the compared results of the transmittance characteristics of the as-deposited samples and the same samples

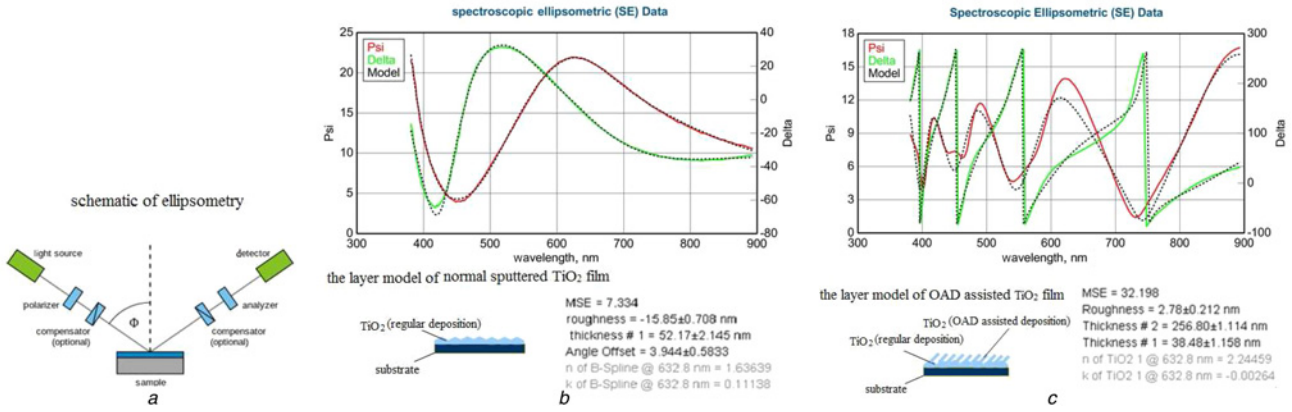

Fig. 6 *Refractive index tested with the ellipsometry method*
a Schematic of ellipsometry
b Normal sputtered TiO_2 film
c TiO_2 film of normal sputter 2 h and OAD-assisted sputter 2 h (85°)

annealed at 753 K in air for 2 h. The peaks of the annealed samples showed a blue shift of about 50 nm compared with the as-deposited samples due to the quantum size effects. The deposition times of 2, 3, 4 and 6 h were chosen to achieve the different film thickness, and the relationship of transmittance with the thickness was shown in Fig. 4*c*. Fig. 4*d* exhibited the TiO_2 coatings deposited at the different incident angles and deposition time length. For a given deposition-angled module, no apparent difference between the highest transmittance and the wavelength range was observed. In Figs. 4*c* and *d*, there can be concluded that though the thickness of as-deposited films may be increased with the longer deposition times, but the transmittance did not show a significant increase, resulting in increased production costs.

The previous work has demonstrated that thin-film TiO_2 optical coatings can be characterised rapidly and unambiguously by the non-intrusive technique of Raman vibrations. Raman spectroscopy was used in chemistry to provide a structural fingerprint by which molecules can be identified (Raman Spectrometer (BWS 415-785H, B&W TEK Opto-electronics (Shanghai) Co., Ltd.), as shown in Fig. 5.

To obtain further detailed information on the crystallisation of the TiO_2 thin films after heat treated, Raman spectra of TiO_2 samples produced under different heat-treated conditions were conducted at room temperature. Raman spectra were excited using 300 mW of 785.0 nm radiation from a 30 mW solid-state laser. According to the Raman spectrum result, it did not give any specific peaks even after the samples annealed at a series of heat-treatment temperature. The Raman line assignments were not in agreement with those of [22, 23]: the Raman microprobe spectra of natural brookite powder had a characteristic intense band at 153 cm^{-1}, anatase had a band of similar intensity at 144 cm^{-1} and rutile had the five intense lines at 236, 440, 515, 589 and 650 cm^{-1} [22, 23]. The Raman spectrum of TiO_2 reveals that the as-deposited TiO_2 ARC still exhibited the amorphous structure as shown in Fig. 5. The relative intensity of the Raman lines exhibits only modest variation with excitation photon energy. This result told us that the annealing process has few influences on the crystallisation of the TiO_2 coatings fabricated with sputter technique. These phenomena were consistent with the conclusions of other researchers that the TiO_2 film fabricated with RF sputtered was amorphous [24–26]. Deposition rate may play an important role in controlling surface diffusion and atom relocation. It stands to reason that high temperatures and low deposition rates would allow ad-particles to diffuse over greater lengths.

The AR properties of the fabricated surfaces were verified optically by ellipsometry (alpha-SE, J.A. Woollam Co.). The refractive index was calculated according to the Forouhi–Bloomer dispersion equations. The wavelength dependency of the films optical constants has been examined by variable angle spectroscopic ellipsometry (alpha-SE, J.A. Woollam Co.) at the 70° incidence angle in the wavelength range between 380 and 900 nm, using a helium–neon laser as the light source, as shown in Figs. 6*a*–*c*. Ellipsometry is an indirect method that the measured Ψ (display style: psi) and Δ (display style: delta) cannot be converted directly into the optical constants of the sample [27, 28]. Δ is the phase difference that develops between the s- and p-wave components after reflection. The quantity tan Ψ is related to the amplitude ratio.

Two physical models were developed in order to describe physically possible TiO_2 films. The normal sputtered TiO_2 films, assumed to be ideally homogeneous, were first described by a single-layer model (Fig. 6*b*). The second model for TiO_2 films [normal sputter 2 h and OAD-assisted sputter 2 h (85°)] are a double-layer film with a dense TiO_2 layer and a surface roughness layer (Fig. 6*c*), based on the island film formation. Models were based physically on energy transitions or simply free parameters used to fit the data. The obtained thickness values were 52.17 ± 2.145 nm (the normal sputtered TiO_2 film) and 256.8 ± 1.114 nm [the TiO_2 film of OAD-assisted sputter 2 h (85°)], as shown in Figs. 6*b* and *c*. The values of refractive index n (632.8 nm) for the TiO_2 coating was 1.636 in normal sputter sample, 2.245 in normal and OAD-assisted sputter sample, which was lower than the dense film such as anatase ($n = 2.49$), brookite ($2.58 < n < 2.70$) and rutile ($n = 2.903$). The effective refractive index was a direct consequence of the material–air composite and can be approximated by effective medium theories. The results demonstrated that the graded-index coating had low reflectivity that leads to significant improvement in optical performance and to new microoptics capabilities.

4. Conclusion: In nanotechnology, the most common way to suppress reflection is to apply thin films to a substrate, to modify the surface with a suitable pattern or to introduce a porous material to the surface. We experimentally demonstrate that the high refractive index of TiO_2 material can be decreased to 2.24 using the technique of magnetic sputter combined with OAD. It dramatically reduces the reflectance and enhances the transmittance in the visible light regions. To approach conditions existing during vacuum evaporation and promote tilted nano-textured structure growth, MSP deposition at different deposited angles or at different target–substrate distances had been optimised. The best transmittances of TiO_2 were deposited at 85° angled module and the target–substrate distances of 85 mm in 2 h normal sputter and another 2 h OAD-assisted sputter. It still kept the amorphous state even after 2 h high-temperature annealing. With the current trend of technology moving toward optically transparent

doi: 10.1049/mnl.2017.0408

for the application of AR technology, the high refractive index material of TiO_2, due to its environmentally benign processing methods, has achieved the obvious advantages. Continuing work on oriented sputter-deposited films is in progress.

5. Acknowledgments: The authors are grateful to Dr. Siqi Zhang for performing the ellipsometry measurements. This research was performed in the framework of a financed fund by Shanghai Institute of Space Power-Sources (grant no. 2014-YF-0420).

6 References

[1] Li X., Li P.-C., Ji L., *ET AL.*: 'Subwavelength nanostructures integrated with polymer-packaged III–V solar cells for omnidirectional, broad-spectrum improvement of photovoltaic performance', *Prog. Photovolt., Res. Appl.*, 2015, **23**, pp. 1398–1405

[2] Lindroos J., Savin H.: 'Review of light-induced degradation in crystalline silicon solar cells', *Sol. Energy Mater. Sol. Cells*, 2016, **147**, pp. 115–126

[3] Deng C., Ki H.: 'Pulsed laser deposition of refractive-index-graded broadband antireflection coatings for silicon solar cells', *Sol. Energy Mater. Sol. Cells.*, 2016, **147**, pp. 37–45

[4] Sikder U., Mohammad A.Z.: 'Optimization of multilayer antireflection coating for photovoltaic applications', *Opt. Laser Technol.*, 2016, **79**, pp. 88–94

[5] Stern M.B.: 'Binary optics: a VLSI-based microoptics technology', *Microelectron. Eng.*, 1996, **32**, pp. 369–388

[6] Veldkamp W.B.: 'Binary optics: a new approach to optical design and fabrication', *Opt. News*, 1988, **14**, (12), pp. 29–30

[7] Li D., Carette M., Granier A., *ET AL.*: 'In situ spectroscopic ellipsometry study of TiO_2 films deposited by plasma enhanced chemical vapour deposition', *Appl. Surf. Sci..*, 2013, **283**, pp. 234–239

[8] Raut H.K., Anand Ganesh V., Sreekumaran Nair A., *ET AL.*: 'Anti-reflective coatings: a critical, in-depth review', *Energy Environ. Sci.*, 2011, **4**, pp. 3779–3804

[9] Guldin S., Kohn P., Stefik M., *ET AL.*: 'Self-cleaning antireflective optical coatings', *Nano Lett.*, 2013, **13**, (11), pp. 5329–5335

[10] Buskens P., Burghoorn M., Maurice C.D.M., *ET AL.*: 'Antireflective coatings for glass and transparent polymers', *Langmuir*, 2016, **32**, (27), pp. 6781–6793

[11] Barranco A., Borras A., Gonzalez-Elipe A.R., *ET AL.*: 'Perspectives on oblique angle deposition of thin films: from fundamentals to devices', *Prog. Mater. Sci..*, 2016, **76**, pp. 59–153

[12] Xi J.Q., Schubert M.F., Kim J.K., *ET AL.*: 'Optical thin-film materials with low refractive index for broadband elimination of Fresnel reflection', *Nat. Photonics*, 2007, **1**, pp. 176–179

[13] Pudasaini P.R., Ayon A.A.: 'High efficiency nanotextured silicon solar cells', *Opt. Commun.*, 2012, **285**, pp. 4211–4214

[14] Pudasaini P.R., Elam D., Ayon A.A.: 'Aluminum oxide passivated radial junction sub-micrometre pillar array textured silicon solar cells', *J. Phys. D, Appl. Phys.*, 2013, **46**, (23), pp. 235104–235111

[15] Zhang J., Li Y., Zhang X., *ET AL.*: 'Colloidal self-assembly meets nanofabrication: from two dimensional colloidal crystals to nanostructure arrays', *Adv. Mater.*, 2010, **22**, pp. 4249–4269

[16] Jayasinghe R.C., Perera A.G.U., Zhu H., *ET AL.*: 'Optical properties of nanostructured TiO_2 thin films and their application as antireflection coatings on infrared detectors', *Opt. Lett.*, 2012, **37**, (20), pp. 4302–43042

[17] Li T., Zhiqiang M., Min W., *ET AL.*: 'Sub-wavelength structure polyimide anti-reflection film with the technique of nano-imprint lithography (NIL)', *J. Harbin Inst. Technol.*, 2016, **48**, (10), pp. 66–70

[18] Li M., Shen H., Zhuang L., *ET AL.*: 'SiO_2 antireflection coatings fabricated by electron-beam evaporation for black monocrystalline silicon solar cells', *Int. J. Photoenergy*, 2014, (2014) Article ID 670438, 5 pages

[19] Bian Y., Wang X., Zeng Z., *ET AL.*: 'Preparation of ordered mesoporous TiO_2 thin film and its application in methanol catalytic combustion', *Surf. Interface Anal.*, 2013, **45**, pp. 1317–13223

[20] Tian L., Wang W., Zhai Q., *ET AL.*: 'Gradient-index TiO_2 transflector on SiO_2 substrate by magnetron sputtering combining with oblique angle deposition technique'. Third NANOSMAT-USA Int. Conf., ArlinGton, TX, 18–20 May 2016. unpublished

[21] https://en.wikipedia.org/wiki/Transmittance, accessed 15 May 2017

[22] Iliev M.N., Hadjiev V.G., Litvinchuk A.P.: 'Raman and infrared spectra of brookite (TiO_2): experiment and theory', *Vib. Spectrosc.*, 2013, **64**, pp. 148–152

[23] Narayanan P.S.: 'Raman spectrum of rutile (TiO_2)', *Proc. Indian Acad. Sci. A*, 1950, **32**, pp. 279–283

[24] Eufinger K., Janssen E.N., Poelman H., *ET AL.*: 'The effect of argon pressure on the structural and photocatalytic characteristics of TiO_2 thin films deposited by d.c. magnetron sputtering', *Thin Solid Films*, 2006, **515**, pp. 425–429

[25] Exarhos G.J.: 'Substrate signal suppression in Raman spectra of sputter deposited TiO_2 films', *J. Chem. Phys.*, 1984, **81**, (11), pp. 5211–5213

[26] Sathiaraj T.S.: 'Optical constants of RF sputtered amorphous TiO_2 films [J]', 2004, **29**, pp. 1455–1458

[27] Li D., Carette M., Granier A., *ET AL.*: 'Spectroscopic ellipsometry analysis of TiO_2 films deposited by plasma enhanced chemical vapor deposition in oxygen/titanium tetraisopropoxide plasma', *Thin Solid Films*, 2012, **522**, pp. 366–371

[28] Eiamchai P., Chindaudom P., Pokaipisit A., *ET AL.*: 'A spectroscopic ellipsometry study of TiO_2 thin films prepared by ion-assisted electron-beam evaporation', *Curr. Appl. Phys.*, 2009, **9**, pp. 707–712